Determination of the Hydrocarbon Core Structure of Fluid Dioleoylphosphocholine (DOPC) Bilayers by X-Ray Diffraction Using Specific Bromination of the Double-Bonds: Effect of Hydration

Kalina Hristova and Stephen H. White
Department of Physiology and Biophysics, University of California, Irvine, California 92697-4560 USA

ABSTRACT Changes in the structure of the hydrocarbon core (HC) of fluid lipid bilayers can reveal how bilayers respond to the partitioning of peptides and other solutes (Jacobs, R. E., and S. H. White. 1989. *Biochemistry.* 28:3421–3437). The structure of the HC of dioleoylphosphocholine (DOPC) bilayers can be determined from the transbilayer distribution of the double-bonds (Wiener, M. C., and S. H. White. 1992. *Biophys. J.* 61:434–447). This distribution, representing the time-averaged projection of the double-bond positions onto the bilayer normal (z), can be obtained by means of neutron diffraction and double-bond specific deuteration (Wiener, M. C., G. I. King, and S. H. White. 1991. *Biophys. J.* 60:568–576). For fully resolved bilayer profiles, a close approximation of the distribution could be obtained by x-ray diffraction and isomorphous bromine labeling at the double-bonds of the DOPC *sn*-2 acyl chain (Wiener, M. C., and S. H. White. 1991. *Biochemistry.* 30:6997–7008). We have modified the bromine-labeling approach in a manner that permits determination of the distribution in under-resolved bilayer profiles observed at high water contents. We used this new method to determine the transbilayer distribution of the double-bond bromine labels of DOPC over a hydration range of 5.4 to 16 waters per lipid, which reveals how the HC structure changes with hydration. We found that the transbilayer distributions of the bromines can be described by a pair of Gaussians of 1/e half-width A_{Br} located at $z = \pm Z_{Br}$ relative to the bilayer center. For hydrations from 5.4 waters up to 9.4 waters per lipid, Z_{Br} decreases from 7.97 ± 0.27 Å to 6.59 ± 0.15 Å, while A_{Br} increased from 4.62 ± 0.62 Å to 5.92 ± 0.37 Å, consistent with the expected hydration-induced decrease in HC thickness and increase in area per lipid. After the phosphocholine hydration shell was filled at ~12 waters per lipid, we observed a shift in Z_{Br} to ~7.3 Å, indicative of a distinct structural change upon completion of the hydration shell. For hydrations of 12–16 waters per lipid, the bromine distribution remains constant at Z_{Br} = 7.33 ± 0.25 Å and A_{Br} = 5.35 ± 0.5 Å. The absolute-scale structure factors obtained in the experiments provided an opportunity to test the so-called fluid-minus method of structure-factor scaling. We found that the method is quite satisfactory for determining the phases of structure factors, but not their absolute values.

INTRODUCTION

The physical state of a fluid L_α-phase lipid bilayer is mirrored by the organization and motions of the acyl chains comprising its hydrocarbon core (HC). This is clearly revealed by the decreases in HC thickness (Levine and Wilkins, 1971; Torbet and Wilkins, 1976) and ^{2}H-NMR alkyl-chain order parameters (Boden et al., 1991; Koenig et al., 1997) that accompany increases in hydration. Similar effects are seen when peptides partition into bilayer interfaces and thereby increase the area per lipid (Jacobs and White, 1987, 1989; Wu et al., 1995). Measures of the structure of the HC are thus useful for understanding molecular interactions that depend upon the structure and stability of bilayers. We show here that x-ray diffraction measurements of the transbilayer distribution of bromine-labeled double-bonds in 1,2-dioleoyl-*sn*-glycero-3-phosphocholine (dioleoylphosphocholine; DOPC) bilayers provide a useful measure of HC structure that is remarkably sensitive to structural changes, induced in the present case by changes in hydration.

Double-bonds in phospholipid acyl chains cause bilayers to be in a fluid state at biologically relevant temperatures [reviewed by Small (1986)], especially when located in the middle of the chain (Barton and Gunstone, 1975), which is the usual case for naturally occurring monounsaturated phospholipids. For DOPC bilayers at 66% relative humidity (RH) (5.4 waters/lipid), Wiener and White (1992) showed that the transbilayer distribution of the thermally disordered double-bonds provide a measure of the thickness of the HC as well as its thermal disorder. This distribution, defined as the time-averaged positions of the double-bonds projected on to the bilayer normal, was determined exactly by neutron diffraction using DOPC specifically deuterated at the double-bonds (Wiener et al., 1991) and approximately by x-ray diffraction using DOPC specifically brominated at the double-bonds of the *sn*-2 chain (Wiener and White, 1991c). The latter distribution differs from the true one only by being slightly broader (~0.7 Å) due to the size of the bromines. Here we demonstrate the feasibility of using the bromine labeling method as a means of monitoring changes in HC structure. Specifically, we have determined the time-averaged transbilayer distribution of the bromine labels in bilayers formed from isomorphous mixtures (Wiener and White, 1991c) of DOPC and 1-oleoyl-2-(9, 10-dibromoste-

Received for publication 8 October 1997 and in final form 8 February 1998.

Address reprint requests to Stephen H. White, Department of Physiology and Biophysics, University of California, Irvine, CA 92697-4560. Tel.: 714-824-7122; Fax: 714-824-8540; E-mail: shwhite@uci.edu.

0006-3495/98/05/2419/15 $2.00

aroyl)-*sn*-glycero-3-phosphocholine (OBPC) over a hydration range of 5.4 to 16 waters per lipid. We show that the transbilayer distributions of the bromines over the full range of hydration can be described by a pair of Gaussian functions of 1/e half-width A_{Br} located at $z = \pm Z_{Br}$ relative to the bilayer center, and that these distributions are sensitive measures of the state of the HC.

This work is part of an ongoing investigation of the use of so-called "liquid-crystallography" (Wiener and White, 1991a, b) for the determination of the structure of liquid-crystalline bilayers using refinement methods commonly used in protein crystallography [reviewed by White and Wiener (1995, 1996)]. Therefore, an additional goal was to extend the liquid-crystallographic method to high hydrations where its application can be problematic (see below). The structural images of fluid bilayers obtained by liquid-crystallography account for all of the mass of the unit cell by subdividing the phospholipids and water within it into a series of "quasimolecular fragments" (King and White, 1986) such as the carbonyls, phosphates, cholines, etc. The "structure" of each fragment consists of the time-averaged projection of the three-dimensional motion of the fragment onto the bilayer normal. Because of the central-limit theorem (Barlow, 1989), these projections are invariably Gaussian distributions, as observed experimentally (Wiener et al., 1991; Wiener and White, 1991c). The complete bilayer structure consists of the full set of these distributions. In the present work, we have determined only one of these distributions, the double-bonds.

Liquid-crystallography was originally developed using experimental data from highly oriented lipid multilayers that form nearly perfect one-dimensional lattices at low hydrations. At high hydrations, orientational disorder, thermal motion, and membrane undulations (Sirota et al., 1988; Nagle et al., 1996; Zhang et al., 1996) can decrease the number of observable diffraction orders h_{obs} and thereby limit the use of the method (Wiener and White, 1992). Indeed, we found in the course of the present studies that h_{obs} dropped from 8 at 5.4 waters/lipid to an impractical 3 orders for more than 16 waters/lipid. A modification of the original x-ray data-scaling method (Wiener and White, 1991c), described in detail in Methods, allowed determination of the distribution of the bromine labels with as few as 4 orders of data.

For perfect crystals, one's ability to resolve the atoms of the unit cell is limited only by the thermal motions of the atoms which are taken into account in the refined structural model by means of the Debye-Waller formalism (Warren, 1969). These thermal motions limit the number of diffraction orders that can be observed to a value defined as h_{max}. The characteristic spatial extent of thermally disordered atoms or small clusters of atoms is approximately d/h_{max}, where d measures the unit cell size (Wiener and White, 1991a). For example, atoms smeared over a space of ~2 Å in a bilayer unit cell with $d = 50$ Å will produce ~25 orders of diffraction (Sakurai et al., 1977; Suwalsky and Duk, 1987). Such a unit cell is intrinsically a *high-resolution* structure. In contrast, the unit cell of the liquid-crystalline bilayer is so highly thermally disordered that only a few diffraction orders are possible (typically $h_{max} = 5$–10) because the atoms are smeared together into large quasimolecular clusters with spatial extents of 5–10 Å. Such unit cells are intrinsically *low-resolution* structures. However, no matter what the intrinsic resolution of a unit cell is, collection of all of the h_{max} diffraction orders will produce a *fully resolved* (accurate) image of the structure. For high thermal disorder, the image will be a fuzzy one. Nevertheless, an accurate image of the fuzzy structure can be obtained.

The collection or analysis of fewer than the h_{max} possible diffraction orders will result in an *under-resolved* (inaccurate) image of the structure [see Wiener and White (1991a)]. Two types of disorder, orientational and lattice, can lead to under-resolved images of fluid bilayers. If lipid multilayers are highly oriented, i.e., the bilayer lamellae are flat and their normals are coincident, the diffraction peaks are essentially images of the incident x-ray beam so that the signal-to-noise ratio is maximized. But, if the multilayers have a range of orientations, i.e., the bilayer lamellae are curved, the diffraction peaks will be smeared into arcs (circles in the case of completely random orientations such as in simple multilamellar dispersions). This smearing can reduce the high-order diffraction peaks to below the noise level and thereby cause h_{obs} to be smaller than h_{max}. Typically, orientational disorder can cause $h_{obs} \approx h_{max}/2$ for randomly oriented samples. Lattice disorder also can reduce the number of observable diffraction orders because the loss of spatial coherence leads to a progressive broadening of diffraction peaks as h increases (Hosemann and Bagchi, 1962). High lattice disorder can therefore cause the intensities of high-order peaks to fall below the noise level. For highly oriented samples, one must therefore establish that $h_{obs} = h_{max}$ in order to be certain that a structure is fully resolved. This can be done by measuring the widths of the diffracted peaks as a function of h provided that the x-ray optics are not limiting [see Wiener and White (1991a)]. Even then, there is the possibility of the existence of high-order structure factors that cannot be detected because they are below the noise level of the detector (Wiener and White, 1991b). The Monte Carlo refinement procedure of Wiener and White (1992) accounts for this possibility.

The above discussion shows that liquid-crystallography can be problematic at high hydrations because the combined effects of orientational and lattice disorder can cause $h_{obs} < h_{max}$. The primary cause of lattice disorder in bilayer systems at high hydrations is likely to be undulations (Helfrich, 1973) if the lamellae are sufficiently flexible (Sirota et al., 1988). Unlike the thermal fluctuations, which occur relative to a bilayer's mean position, undulations are fluctuating whole-body motions of the bilayers. Besides introducing lattice disorder, they can cause an additional smearing (broadening) of the Gaussian distributions that describe the thermal motion of the quasimolecular fragments. The presence of undulations is detected through high-resolution

measurements of the shapes of the diffracted intensities (Sirota et al., 1988; Nagle et al., 1996; Zhang et al., 1996). Such measurements were not feasible for the present work. As an alternative, we used a simple modeling approach to examine the likelihood of undulations being the cause of the reduction in h_{obs} at higher hydrations. The analysis, presented in the Discussion, indicates that undulations are not a serious problem over the range of 5.4 to 16 waters/lipid.

MATERIALS AND METHODS

Materials

DOPC and OBPC were purchased from Avanti Polar Lipids (Alabaster, AL). Purity of OBPC was determined by elemental analysis to be >99.9% (Microlit Laboratories, Madison, NJ). Polyvinylpyrrolidone, M_r = 40,000 (PVP) with an average molecular weight of 40,000 and intrinsic viscosity of 28–32, designated as PVP-40, was purchased from Sigma Chemical Co. (St. Louis, MO).

Sample preparation

Oriented samples

Oriented samples were prepared on curved glass substrates using methods adapted from Franks and Lieb (1979), Jacobs and White (1989), and Wiener and White (1991c). Appropriate aliquots of DOPC and OBPC with a combined mass of ~2 mg were mixed in chloroform to achieve a desired molar ratio. Methanol was added to the solution to obtain a $CHCl_3$:MeOH volumetric ratio of 1:1 and the solution vortexed. The widest part of a 3.5-mm glass x-ray capillary (Charles Supper Co., Natick, MA), diameter ~5 mm, was cut with a gas microtorch and then mounted on the shaft of a rotary vacuum-evaporator motor that spun the tube about its long axis at ~140 rpm during sample application. The lipid solution was applied dropwise with a 25 μl syringe (Hamilton Co., Reno, NV) on the outer surface of the rotating tube to obtain a uniform layer. Spinning of the tube continued until most of the solvent had evaporated. All traces of the solvent were removed under vacuum. The sample was placed in a custom-made sample chamber with two thin beryllium windows adapted to a small goniometer. The relative humidity (RH) inside the chamber was controlled by saturated salt solutions (O'Brien, 1948; ASTM Standards, 1952) in small tubes adjacent to the sample. The chamber has two valves that allow it to be flushed with an inert gas (argon or helium) to prevent lipid oxidation. To assure equilibrium before mounting the sample in the x-ray beam, the entire chamber with valves open was placed in a sealed container containing a large volume of saturated salt solution. After the sample was equilibrated overnight under argon, the jar was opened, the valves were quickly closed, and the chamber mounted on the main goniometer head. X-ray exposure times were between 12 and 24 h. The sample tube was arranged such that the incident x-rays were tangent to the curved surface of the oriented multilayer at a glancing angle so that all of the lamellar diffraction orders could be recorded at a fixed value of ω. With this geometry, most of the wide-angle diffraction is absorbed by the glass substrate (Wiener and White, 1991c). Data suitable for scaling were collected at relative humidities of 76, 86, and 93% [concentrated salt solutions (ASTM Standards, 1952) of NaCl, KCl, and $NH_4H_2PO_4$, respectively] corresponding to hydrations of 6.2, 7.7, and 9.4 waters/lipid (McIntosh et al., 1989). Data for 66% RH (5.4 waters/lipid) were available from the work of Wiener and White (1991c).

Unoriented samples

Mechanically stable oriented bilayers could be deposited on a substrate only at low hydrations (up to 93% RH, 9.4 waters/lipid). At higher hydrations, unoriented lipid suspensions were used. They were prepared by co-dissolving the DOPC/OBPC lipid mixtures in chloroform as for oriented samples. Most of the chloroform was removed under a stream of nitrogen and the remainder by lyophilization. The dehydrated lipid mixtures were then incubated in buffer (0.1 M NaCl, 10 mM HEPES, pH 7) mixed with PVP solution for several days at 4°C. The osmotic pressures of PVP solutions and their corresponding relative humidities are known (Parsegian et al., 1986). To assure complete equilibration, the lipid suspensions were periodically vortexed and cycled through the DOPC main phase transition temperature of −20°C (Barton and Gunstone, 1975) at least five times. The lipid/PVP suspensions were sealed in 1-mm glass x-ray capillary tubes and mounted on the goniometer head. Exposure times varied between 12 and 24 h. Data suitable for scaling were collected for nominal PVP concentrations of 60, 50, 40, and 30% (w/v), corresponding to hydrations of 12.0, 13.6, 14.2, and 15.9 waters/lipid, respectively (McIntosh et al., 1989).

Sample degradation

Sample degradation was monitored by TLC. For typical exposure times of 1–2 days, no degradation was detected. Furthermore, no systematic differences in the line widths or integrated intensities were observed between samples of the same hydration.

Collection of x-ray intensities and integration of peaks

X-ray diffraction experiments were performed with Ni-filtered CuK_α radiation on an 18 kW Siemens (Madison, WI) rotating anode x-ray generator operated at 38 kV and 40 mA (1.52 kW). The beam was collimated and focused at the 2D detector array using double-mirror optics (Charles Supper, Natick, MA). Diffraction patterns were recorded on a Siemens X-1000 xenon-filled area detector with position decoding circuit and real-time data display. A displayed data frame consisted of typical lamellar diffraction patterns appropriate for oriented and unoriented samples that consisted of curved arcs around the χ-axis with lamellar spacings along the 2θ radial. The initial processing of the data from the position decoding circuit was performed using the Siemens General Area Detector Diffraction Software (GADDS). For each data set analyzed, $\Delta\chi \times \Delta 2\theta$ wedge-shaped "sectors" were chosen manually to include the diffracted intensities that were then summed around the χ-axis (i.e., along the arcs of the diffraction peaks) using the GADDS "bin" method. The result of the χ integration is the total diffracted intensity versus the Bragg angle, 2θ. Using this procedure, the observed structure factors for both oriented and unoriented samples are given by

$$f(h) = \sqrt{I(h)A(h)h} \quad (1)$$

where $I(h)$ is the intensity of the hth peak and $A(h)$ is the absorption correction (see below).

For oriented samples the mosaic spreads never exceeded 30°, but were generally much smaller, 5° or less. Very long exposures demonstrated that for oriented samples $h_{obs} = h_{max}$. Because the first-order peak was much stronger and wider due to its very high intensity, the integration was performed in two steps. The intensities were first integrated around the χ-axis for a wide sector containing all the diffracted intensity to be certain that all of the very intense first order was collected. For this wide sector, the high-order peaks were lost in the noise because of the long length of the integration path. The sector was then changed to accommodate only the high-order peaks; the χ-axis integration was performed on a segment that did not include the first order and was much narrower. This reduced the amount of background included in the integration so that even the highest-order diffraction peaks could be easily detected above the noise level. The internal consistency of the two integration procedures was verified by comparing the integrated intensities of the relatively strong 3rd- and 4th-order peaks, which could be analyzed by either method. The intensities agreed within experimental uncertainty.

For unoriented samples, as expected, the integrated intensities did not depend on the width and the orientation of the integration sector. However, no more than four orders could be seen for unoriented samples in PVP solutions. Bulk samples prepared to have hydrations corresponding to those of 66 to 93% RH also gave only four diffraction orders because the weak high-order peaks were spread over a larger detector area and consequently had lowered signal-to-noise ratio (see Discussion).

After the χ integration, the $I(2\theta)$ peaks were analyzed using the software package Origin™ (MicroCal, Inc., Northampton, MA) in the following way: first, the peaks were deleted, leaving only the background, which was then fit with a polynomial function. This fitted background was subtracted from the original data leaving only the diffraction peaks. The peaks were integrated in Origin™ using two different methods: numerical integration of the areas under the peaks or by fitting Gaussians to the diffraction peaks and integrating analytically. The average of the two areas given by the two methods yielded $I(h)$ for use in Eq. 1. The difference between the two areas was usually smaller than the estimated uncertainty of the intensity calculated from (peak area + background)$^{1/2}$. The experimental uncertainties of oriented samples at 76% RH were typical of those observed for all experiments: 0.1% for the intense 1st-order peak, 2% for the strong 4th-order, and 20% for the very weak 2nd-order.

Absorption corrections

Some of the incident and diffracted x-rays are absorbed during passage through oriented samples. The lower orders follow longer total paths and therefore have the larger correction factors. For oriented samples, the adsorption correction is given by Wiener and White (1991c):

$$A(h) = \exp(2\mu r \sin\theta)\int_0^t \exp(-2\mu[(r+\xi)^2 - (r\cos\theta)^2]^{1/2})d\xi \quad (2)$$

where θ is the Bragg angle, $2d \sin\theta = h\lambda$, and μ is the linear absorption coefficient of the lipid. In our experiments μ varied from 8 to 14.2 cm^{-1}. The film thickness, t, was estimated to be in the range 10–20 μm, depending on the weight of the sample. $A(h)$ varied from 1.1 for pure DOPC to 1.3 for 1:1 DOPC:OBPC for $h = 1$. For unoriented samples no adsorption correction was necessary, so that $A(h) = 1$.

Scaling of structure factors

The experimental structure factors $f(h)$ from a given experiment depend upon the amount of sample in the beam, precise geometry of the sample-beam intersection, x-ray beam intensity, and other experimental conditions. The true (absolute) structure factors, $F^*(h)$, are determined solely by the scattering factor of the unit cell. The experimental structure factors are related to the true structure factors by $f(h) = KF^*(h)$, in which K is the instrumental constant. Fourier reconstructions of bilayer scattering-length or electron density profiles yield only arbitrary fluctuations of scattering density along the bilayer normal if $f(h)$ rather than $F^*(h)$ is used. Determination of the instrumental constant allows one to relate the scattering profiles obtained in diffraction experiments to the actual contents and molecular packing of the bilayer unit cell. To do this, one must 1) determine the true mean value of the scattering profile using the composition of the unit cell, and 2) calibrate the fluctuations around this mean value (Franks et al., 1978; Wiener and White, 1991c). This is done by a scaling procedure (Wiener and White, 1991c) summarized below.

The relative absolute scale

Absolute bilayer profiles determined by x-ray diffraction are frequently reported in units of electrons/Å^3, but we prefer scattering-length/Å^3 because electron density is not relevant to neutron scattering (neutrons scatter from atomic nuclei rather than electrons). Furthermore, in the composition-space refinement method that combines x-ray and neutron data (Wiener and White, 1991b; Wiener and White, 1992), the transbilayer probability distribution functions of the quasimolecular fragments are mapped to x-ray and neutron scattering-length spaces by simply scaling them by the scattering length, b. We have thus adopted the convention of using x-ray or neutron scattering-length density rather than electron density (Wiener and White, 1991b; Wiener and White, 1992). X-ray scattering lengths b_X (units: 10^{-12} cm) are obtained from the atomic number n using $b_X = (mc^2/e^2)n$.

The absolute scattering-length density $\rho(z)$ along the bilayer normal z is given by King et al. (1985) and Jacobs and White (1989):

$$\rho(z) = \rho_0 + \frac{2}{d}\cdot\frac{1}{K}\sum_{h=1}^{N} f(h)\cos\left(\frac{2\pi hz}{d}\right) \quad (3)$$

where the $f(h)$ are the measured structure factors in arbitrary units, K is the instrumental constant, d the Bragg spacing, ρ_0 the average scattering-length density of the unit cell, and N the highest observed diffraction order.

Equation 3 assumes that the volume (V) and composition of the unit cell are known. $V = S \cdot d$ where S is the area/lipid. Because S is often not immediately available, we have adopted the so-called relative absolute scale (Jacobs and White, 1989), or *per-lipid* scale, that describes scattering density on a per lipid molecule basis. This is done by simply multiplying both sides of Eq. 3 by S, which yields what we call the "scattering density" (units: scattering-length/length)

$$\rho^*(z) = \rho_0^* + \frac{2}{d}\cdot\frac{1}{k}\sum_{h=1}^{N} f(h)\cos\left(\frac{2\pi hz}{d}\right) \quad (4)$$

where $\rho^*(z) = \rho(z)S$, $\rho_0^* = \rho_0 S$, and $k = K/S$. With these definitions, the relative absolute structure factors are given by $F^*(h) = f(h)/k$.

Scaling principles

The average scattering density ρ_0^* of the unit cell is obtained from the scattering lengths of the molecules within the unit cell by means of the equation (Jacobs and White, 1989)

$$\rho_0^* = \frac{2}{d}(n_w b_w + b_{lip}) \quad (5)$$

where n_w is the number of waters/lipid, b_w the water scattering length, and b_{lip} the scattering length of a single lipid molecule.

As noted earlier, scattering density profiles constructed from the $f(h)$ alone yield arbitrary fluctuations of the scattering density around the mean value ρ_0^*. The scale factor k scales the amplitude of these fluctuations to the relative absolute fluctuations. It is determined by introducing a strongly scattering "label" (e.g., bromine) of known scattering length into the unit cell without changing the unit cell structure (isomorphous replacement) and then determining the so-called difference structure. In the present experiments we labeled the double-bond of the *sn*-2 chain of DOPC with 2 bromines to produce OBPC (see Materials) which is isomorphous with DOPC (Wiener and White, 1991c). In general, one replaces a fraction x of the DOPC with OBPC that has scattering length $b_{lip} + 2b_{Br}$ where b_{Br} is the scattering length of bromine. Using Eq. 4, the average scattering density of the unit cell becomes

$$\rho_0^*(x) = \frac{2}{d}(n_w b_w + b_{lip} + 2xb_{Br}) \quad (6)$$

In the simplest difference-structure experiment, one determines the structure factors $f(h)$ of a pure DOPC bilayer and the structure factors $f_x(h)$ of bilayers containing a fraction x of OBPC. If the instrumental constant k

is exactly the same in the two experiments, then, from Eq. 3, the difference structure is given by

$$\Delta\rho^*(z) = \Delta\rho_0^* + \frac{2}{d}\cdot\frac{1}{k}\sum_{h=1}^{N}[f_x(h) - f(h)]\cos\left(\frac{2\pi hz}{d}\right) \quad (7)$$

where $\Delta\rho_0^* = 2xb_{Br}$. The difference structure $\Delta\rho^*(z)$ describes the transbilayer distribution of the bromines and hence the double-bonds. The instrumental constant can be determined if there are regions of the unit cell, such as the water region, that are never visited by the bromines. At any point z_i that is free of bromine, $\Delta\rho^*(z_i) = 0$. Hence,

$$-2xb_{Br} = \frac{2}{d}\cdot\frac{1}{k}\sum_{h=1}^{N}[f_x(h) - f(h)]\cos\left(\frac{2\pi hz_i}{d}\right) \quad (8)$$

from which k can be determined.

The transbilayer distribution of the double-bonds (bromines) is described by a pair of Gaussian distributions of 1/e half-width A_{Br} located at $z = \pm Z_{Br}$:

$$\Delta\rho^*(z) = \frac{2xb_{Br}}{A_{Br}\sqrt{\pi}}\left\{\exp\left[-\left(\frac{z - Z_{Br}}{A_{Br}}\right)^2\right] + \exp\left[-\left(\frac{z + Z_{Br}}{A_{Br}}\right)^2\right]\right\} \quad (9)$$

The parameters of the Gaussians can be determined by using nonlinear least-squares analysis by noting that the Fourier transformation of Eq. 9 yields structure factors that must be equal to the experimentally determined structure factors (Wiener et al., 1991). That is,

$$\frac{1}{k}[f_x(h) - f(h)] = \Delta F_x^*(h) = 2xb_{Br}\exp(-[\pi A_{Br}h/d]^2)\cos(2\pi hZ_{Br}) \quad (10)$$

Scaling procedures

Although the principles of the scaling of the experimental data are simple, experimental reality introduces complications. One must actually examine a number of samples with different fractions of OBPC in order to assure that OBPC is isomorphous with DOPC for all hydrations. If the difference structure factors $\Delta F_x^*(h)$ are linear in x, then the replacement is isomorphous. An additional advantage of this procedure is that it averages out random error. The difficulty is that the amount of sample in the beam, beam intensity, etc., are different for each x so that each experiment has its own instrumental constant k_x. Wiener and White (1991c) have described in detail a procedure for scaling multiple data sets that involves, in simple terms, re-scaling the structure factors so that the data sets are described by a set of internally consistent experimental constants. Their analysis indicated, based upon the availability of $h_{obs} = h_{max} = 8$ diffraction orders, that the multiple-data-set scaling could be accomplished for $h_{max} \geq 3$. In the present experiments, $h_{obs} < h_{max}$ for the high-hydration experiments using unoriented samples. The practical scaling difficulty encountered as a result was that the Fourier reconstructions (Eq. 4) are under-resolved and thus show so-called Fourier noise (Gibbs, 1898a, b). (An example is shown in Fig. 4 *B*.) The principle of calculating the instrumental constant described in the discussion of Eqs. 7 and 8 requires that there be a z_i for which $\Delta\rho^*(z_i) = 0$. Finding such values of z_i is easy if a scattering density profile is fully resolved, but difficult in the presence of Fourier noise because the profiles do not smoothly superimpose in the bromine-free regions. The following modification to the approach of Wiener and White (1991c) allows one to scale multiple data sets provided that $h_{obs} \geq 4$.

Let the relative-absolute structure factors of pure OBPC bilayers be $F_A^*(h)$ and those of pure DOPC bilayers be $F_B^*(h)$. Because the two bilayers are isomorphous, the absolute structure factors for a bilayer with fraction x of OBPC will be

$$F_x^*(h) = xF_A^* + (1 - x)F_B^* \quad (11)$$

$F_A^*(h)$ and $F_B^*(h)$ comprise the basis-set structure factors from which the structure factors $F_x^*(h)$ can be generated. However, $F_A^*(h)$ and $F_B^*(h)$ are not required to be pure DOPC and OBPC. In our case, they were DOPC and 1:1 DOPC/OBPC.

From the several sets of experimental structure factors with unnormalized instrumental constants, the method of Wiener and White (1991c) establishes a set of self-consistent internally normalized instrumental constants such that Eq. 11 can be written

$$\frac{f_x(h)}{k_x} = x\frac{f_A(h)}{k_A} + (1 - x)\frac{f_B(h)}{k_B} \quad (12)$$

The scattering density profiles $\rho_A^*(z)$ and $\rho_B^*(z)$ can be calculated from Eq. 4 using the appropriate structure factors of Eq. 12. These "basis" profiles are connected through the simple relationship

$$\rho_A^*(z) = \rho_B^*(z) + \rho_{Br}^*(z) \quad (13)$$

where $\rho_{Br}^*(z)$ is the scattering density profile for the bromines. If the profiles are fully resolved, the two experimental constants k_A and k_B can be determined from the system of equations

$$\rho_A^*(z_1) = \rho_B^*(z_1)$$
$$\rho_A^*(z_2) = \rho_B^*(z_2) \quad (14)$$

where z_1 and z_2 are points remote from the bromine scattering peaks in the water region where the profiles can be made to overlap by the proper choice of instrumental constants.

The Wiener-White scaling procedure is built upon Eq. 14. For profiles that are not fully resolved, however, this procedure becomes inaccurate because of Fourier noise. Shown in Fig. 4 *B*, for example, are bromine-distribution difference structures obtained for 14.2 waters/lipid from an unoriented sample with $h_{obs} = 4$. In the water region, roughly from 20 Å to *d/2* from the bilayer center, the Fourier noise is substantial and causes the k_A and k_B to depend on the choice of z_1 and z_2. Although the difference profiles always yielded two Gaussians centered at $z = \pm Z_{Br}$ with 1/e half-width A_{Br}, the Gaussian parameters also depended on the choice of z_1 and z_2. In the modified procedure we took advantage of the fact that the double-bond profiles are invariably Gaussian, as shown by Wiener and White (1991c). That being the case, a fully resolved bromine profile will be described in real and reciprocal space by Eqs. 9 and 10, respectively. If Eq. 7 is rewritten in terms of the basis structure factors, it can be combined with Eq. 13 to yield

$$\frac{2}{d}\sum_{h=1}^{N}\left[\frac{f_A(h)}{k_a} - \frac{f_b(h)}{k_b} - \Delta F_{Br}^*(h)\right]\cos\left(\frac{2\pi hz}{d}\right) = 0 \quad (15)$$

where $\Delta F_{Br}^*(h)$ is $\Delta F_{x=1}^*(h)$ of Eq. 10. The cosines are linearly independent and the sum will be zero only if all coefficients in the brackets in front of the cosines are zero. This results in the system of linearly independent equations

$$\frac{f_A(h)}{k_A} - \frac{f_B(h)}{k_B} = F_{Br}^*(h), \quad h = 1 \ldots h_{obs} \quad (16)$$

By Eq. 10, one can thus write

$$\frac{f_A(h)}{k_A} - \frac{f_B(h)}{k_B} = 2b_{Br}\exp(-[\pi A_{Br}h/d]^2)\cos(2\pi hZ_{Br}), \quad h = 1 \ldots h_{obs} \quad (17)$$

Such a system of h_{obs} equations is obtained for each hydration studied. Equation 17 takes advantage of the fact that one does not need h_{max} difference structure factors to determine the parameters of a Gaussian distribution because the computed and measured difference structure factors will always agree if $h_{obs} \geq 4$ [for an example, see Fig. 2 of Wiener et al. (1991)]. Moreover, the first four structure factors are usually the strongest, and the experimental error in their determination is small. Given a series of measured $f_x(h)$ for a particular hydration, Eqs. 11, 12, and 17 and the general optimization procedure of Wiener and White (1991c) can be used to determine simultaneously k_A, k_B, A_{Br}, and Z_{Br}. The specific computational protocol is as follows:

1. The set of Eqs. (12) is used to linearize all the observed structure factors f. This process yields the instrumental constants for the mixtures of A and B as a function of the scaling constants for A and B and thus places all the data on an internally consistent scale (but not an absolute scale). In addition, the linear regression procedure included in the linearization yields the "best" statistical estimate $\tilde{f}_x(h)$ of the structure factors for a particular fraction x of OBPC.
2. Using the set of Eqs. (17) and the values of $\tilde{f}_A(h)$ and $\tilde{f}_B(h)$ obtained in step 1, k_A, k_B, A_{Br}, and Z_{Br} are determined in a single computational step by "gluing" the two profiles, ρ_A^* and ρ_B^*, in reciprocal space. The procedure is accurate provided that there are at least four orders of diffraction and that all the intensity under each peak is collected (see Discussion). The determination of k_A and k_B yields the relative absolute structure factors $\tilde{f}_A^*(h)$ and $\tilde{f}_B^*(h)$.
3. The instrumental constants k_x, the relative absolute structure factors $F^* = f/k_x$ and their best estimates $\tilde{F}^* = \tilde{f}/k_x$ are determined using Eq. 12 while keeping k_A and k_B fixed.

The results of this protocol are illustrated in Fig. 1, where we present the results of the scaling of the structure factors obtained for six values of x for one particular hydration (86% RH, 7.7 waters/lipid). The data points are the observed relative absolute structure factors F^*. The $\tilde{F}^*$ are found from the parameters of the best-fit straight line passing through the points. Data such as these were obtained for six values of x for each hydration. The error bars are obtained from the statistical uncertainties of the integrated intensities of the diffraction peaks taken as (peak area + background)$^{1/2}$.

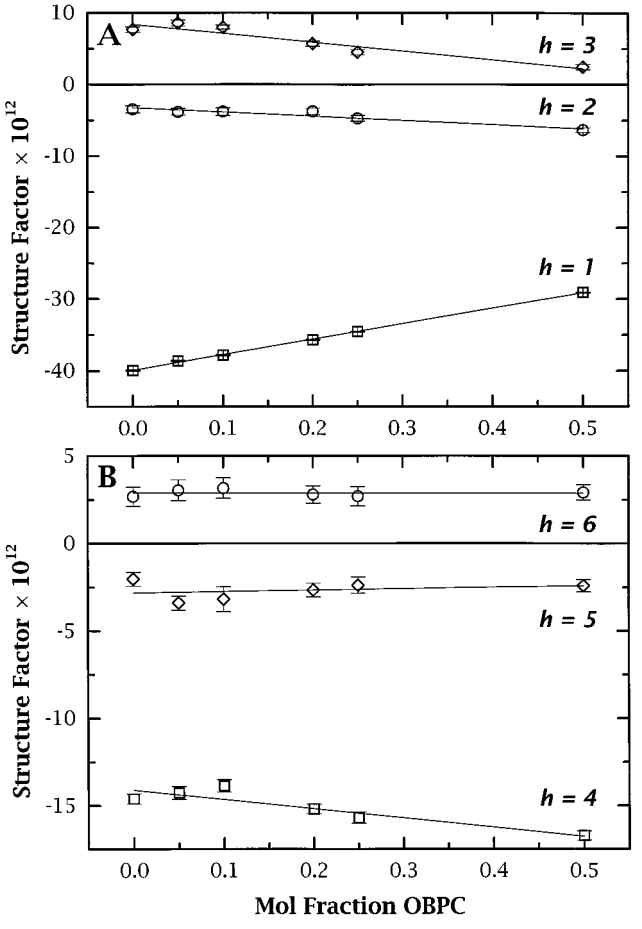

FIGURE 1 Relative-absolute structure factors as a function of mol fraction of OBPC in oriented OBPC/DOPC bilayers for one particular hydration (86% RH, 7.7 waters/lipid). Individual points are the relative absolute structure factors that are related to the arbitrary measured structure factors by instrumental scale factors. The error bars are obtained from the uncertainties in the integrated diffraction peaks. The solid lines are derived from the self-consistent fit to all the data by means of Eq. 12. The values of the solid lines at a given mol fraction OBPC are the best estimates of the relative absolute structure factors, $\tilde{F}^*(h)$.

Estimates of experimental uncertainties in Gaussian parameters

We used the Monte Carlo method of Wiener and White (1992) to estimate the experimental uncertainties of A_{Br}, Z_{Br}, k_A, and k_B. Specifically, Gaussian-distributed noise with a standard deviation equal to the experimental uncertainty in the structure factors was imposed on observed structure factors to produce 10 sets of pseudo structure factors for each hydration. For each of these 10 sets, the entire scaling procedure was performed in order to obtain 10 different estimates of A_{br}, Z_{Br}, k_A, and k_B whose standard deviations from the mean were taken as estimates of the uncertainties.

X-ray phase determination

Specific labeling with bromine allows the determination of the phases of the x-ray structure factors (Franks et al., 1978). All the terms in Eq. 10 except the cosine term are positive-definite, and the sign of the cosine depends on h and Z_{Br}. Thus, the determined value of Z_{Br} defines the phases (signs) of $F_x(h)$. The phases of the structure factors were already determined for 66% RH (Wiener and White, 1991c). To scale the data, we assumed initially that the phases of the observed structure factors do not change with hydration. This proved correct because for each value of h, the slope of $F_x(h)$ was in a direction consistent with the determined Z_{Br}.

RESULTS

We examined oriented DOPC multilayers equilibrated at 34% to 93% RH (3–9.4 waters/lipid) and unoriented liposomal suspensions in 60% to 5% PVP solutions (12–26.1 waters/lipid) containing from 0 to 50 mol % OBPC (six different values for each hydration). As summarized in Table 1, the transbilayer bromine (double-bond) distributions were determined only over the hydration range of 5.4 to 15.9 waters/lipid because the scaling procedure described in Methods could not be applied outside that range. For low hydrations (3–5 waters/lipid), the incorporation of OBPC led to the appearance of two satellite off-axis peaks between the 3rd- and the 4th-order lamellar peaks, indicating that OBPC/DOPC bilayers were not isomorphous with DOPC bilayers. For hydrations above 16 waters/lipid, the scaling could not be performed because too few orders of diffraction could be observed ($h_{obs} \leq 3$). The measured Bragg spacings for five or more waters/lipid did not depend upon the mol % of OBPC at any hydration used, consistent with isomorphous replacement. Fig. 2 shows the Bragg spacing of DOPC bilayers as a function of the number of water

TABLE 1 Summary of experimental results for x-ray diffraction measurements on DOPC multilamellar bilayers including the Gaussian parameters for the transbilayer distribution of the double-bond determined using bromine labeling of the double-bond in the *sn*-2 chain

Hydration Condition*	W/L[#]	$d \pm$ sd[§] (Å)	h_{obs}[¶]	$Z_{Br} \pm$ sd[‖] (Å)	$A_{Br} \pm$ sd** (Å)	$A_{C=C}$[##] (Å)	$\sqrt{\Sigma F^2/d^2} \pm$ sd $\times 10^5$[§§]
34% RH	2.9	48.4 ± 0.5	8	n/d[¶¶]	n/d	n/d	n/d
44% RH	3.5	48.4 ± 0.5	8	n/d	n/d	n/d	n/d
52% RH	4.1	49.1 ± 0.5	8	n/d	n/d	n/d	n/d
66% RH	5.4	49.1 ± 0.4	8	7.97 ± 0.27	4.96 ± 0.62	4.29	9.4 ± 0.8
76% RH	6.2	49.1 ± 0.5	6	7.33 ± 0.18	5.16 ± 0.77	4.52	8.6 ± 1.9
86% RH	7.7	49.8 ± 0.5	6	7.18 ± 0.15	5.46 ± 0.50	4.86	8.8 ± 1.5
93% RH	9.4	49.8 ± 0.5	6	6.59 ± 0.15	5.92 ± 0.37	5.37	7.1 ± 0.8
60% PVP	12.0	50.5 ± 0.6	4	6.61 ± 0.17	5.66 ± 0.58	5.08	8.2 ± 1.1
50% PVP	13.6	52.5 ± 0.5	4	7.43 ± 0.10	5.48 ± 0.31	4.88	8.8 ± 0.5
40% PVP	14.2	53.3 ± 0.7	4	7.27 ± 0.19	5.20 ± 0.35	4.57	8.2 ± 0.7
30% PVP	15.9	53.5 ± 0.6	4	7.27 ± 0.13	5.36 ± 0.23	4.75	7.9 ± 0.3
25% PVP	18.2	55.8 ± 0.5	3	n/d	n/d	n/d	n/d
20% PVP	19.3	57.0 ± 0.8	3	n/d	n/d	n/d	n/d
15% PVP	21.1	57.6 ± 0.4	3	n/d	n/d	n/d	n/d
10% PVP	23.6	60.2 ± 1.1	2	n/d	n/d	n/d	n/d
5% PVP	26.1	62.3 ± 1.2	2	n/d	n/d	n/d	n/d

*Samples hydrated through vapor by equilibration with saturated salt solutions indicated by % RH (oriented samples) and by dispersal in bulk PVP solutions with wt % PVP indicated (unoriented samples). The listed values of PVP concentrations are nominal. The exact values of wt % PVP were determined via refractive index measurements as 58.54 (60% nominal), 46.71, 42.97, 33.63, 23.43, 19.53, 14.39, 8.69, and 5.09 (5% nominal).

[#]Waters per lipid, based upon measurements of McIntosh et al. (1989) using egg PC and our measurements of DOPC obtained with the same method (data not shown). The value for 66% RH is that of White et al. (1987). The difference in hydration between egg PC and DOPC at the hydrations studied is less than the experimental error. The method of McIntosh et al. (1989) is applicable up to at least 16 waters/lipid, shown by comparing x-ray and NMR data (Koenig et al., 1997).

[§]Lamellar Bragg spacing.

[¶]Number of observed orders of lamellar diffraction.

[‖]Position relative to bilayer center of the Gaussian distribution of the double-bond.

**1/e half-width of the Gaussian distribution of the double-bond.

[##]Estimate of the width of the double-bond (see text).

[§§]Value of constant in Eq. 20. See text. The standard deviations were determined from the uncertainties in k_A and k_B (see Methods).

[¶¶]n/d, not determined. See text.

molecules per lipid. The solid squares (■) correspond to bilayer hydrations (Table 1) for which the distribution of the bromine label could be determined ($h_{obs} \geq 4$). The open symbols (▽, ○) indicate, respectively, the low-end and high-end hydrations whose distributions were not determined. There is a distinct break in the curve at 11.6 waters/lipid that corresponds to the point of completion of the phosphocholine hydration shell (LeNeveu et al., 1977; McIntosh et al., 1989). However, because this break coincided with the change in the method of hydration, there was a small possibility that it was an artifact of the protocol change. We tested this possibility through diffraction experiments on mechanically mixed samples of water and lipid that covered the combined hydration range of the two hydration protocols. The break at ~12 waters/lipid was observed under these conditions as well. Therefore, the break must result from a structural change accompanying the completion of the filling of the phosphocholine hydration shell. This is in complete agreement with the conclusions of studies performed in other laboratories that used a single method of hydration (LeNeveu et al., 1977; McIntosh et al., 1987, 1989).

The structure factors of OBPC/DOPC bilayers with $h_{obs} \geq 4$ were scaled and processed as described in Methods to convert them to best estimates ($\tilde{F}^*$) on the relative-absolute scale. These structure factors are presented in Table 2. Two examples of the resulting bilayer scattering density profiles with 0, 5, 10, 20, 25, and 50 mol % OBPC are shown in Fig. 3. Panel *A* is for oriented bilayers (7.7 waters/lipid; 86% RH) with $h_{obs} = 6$ and panel *B* for unoriented bilayers (14.2 waters/lipid; 40% PVP) with $h_{obs} = 4$. These relative-absolute scale profiles describe the scattering on a per-lipid basis (units: scattering length per length). Division of the relative-absolute density by the area per lipid *S* will convert the profiles to the true absolute scale. Note that the profiles for 7.7 waters/lipid (Fig. 3 *A*) have a "sharper" appearance than the profiles for 14.2 waters/lipid (Fig. 3 *B*) because of the larger h_{obs}. This is because the canonical resolution d/h_{obs} is better as a result of the larger number of structure factors available for the oriented bilayers at 7.7 waters/lipid. The two data sets were scaled independently. The fact that the two sets of profiles have about the same scattering density in the headgroup regions is a good indication of consistency in the scaling. We obtained similar results for all hydrations. The two peaks in the profiles, located at ~± 7 Å relative to the bilayer center, increase with increasing amounts of OBPC and are there-

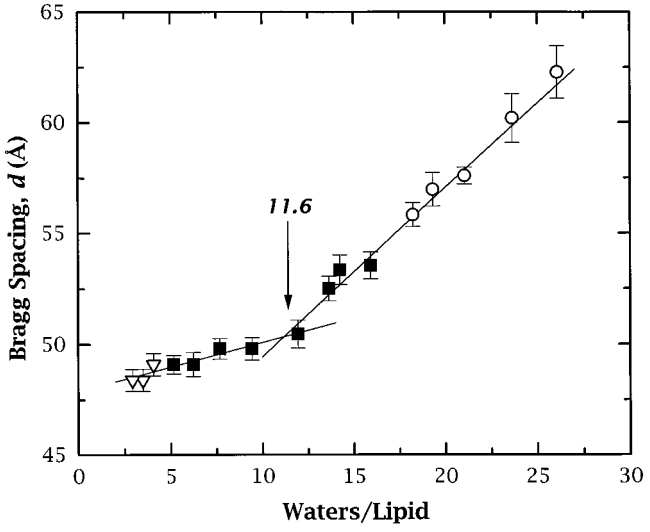

FIGURE 2 Bragg spacing of DOPC bilayers as a function of the number of water molecules per lipid. The break, which occurs at 11.6 water/lipid, corresponds to the point of completion of the hydration shell. This number is in agreement with other studies (LeNeveu et al., 1977; McIntosh et al., 1989). The solid squares (■) correspond to hydrations for which the bromine distribution was determined. The open symbols correspond to hydrations for which the x-ray data do not provide sufficient information to scale the data: for 16–21 waters per lipid only three, and above 22 molecules per lipid only two, diffraction orders were observed (○). For hydrations below 5 molecules per lipid (▽), the OBPC/DOPC bilayers were not isomorphous with the pure DOPC bilayer.

fore identified as the transbilayer distribution of the bromine labels on the double-bond of the *sn*-2 chain.

The difference profiles for 7.7 and 14.2 waters/lipid relative to 0 mol % OBPC, constructed by Fourier synthesis from the difference structure factors (Eq. 7), are presented in Fig. 4, *A* and *B*, respectively. The Fourier ripples in Fig. 4 *B* extending from 20 to 30 Å relative to the bilayer center indicate that the profiles at 14.2 waters/lipid ($h_{obs} = 4$) are under-resolved. As discussed in Methods, Fourier noise such as this made the scaling method of Wiener and White (1991c) inaccurate because it is based upon the assumption of fully resolved profiles. Our modification of the method removes this limitation (see Methods). Note that in Fig. 4 *A* Fourier noise is virtually absent because the images are fully resolved ($h_{obs} = h_{max}$).

Fig. 5, *A* and *B* shows the fully resolved Gaussian distributions of the bromine-labeled double-bonds for 7.7 and 14.2 waters/lipid, respectively, obtained from the scaling procedure described in Methods. A collection of Gaussian distributions covering the range of hydrations are compared in Fig. 6 *A* and the Gaussian parameters A_{Br} and Z_{Br} for all hydrations (5.4 to 15.9 waters/lipid, Table 1) are plotted against hydration in Fig. 6 *B*. For hydrations from 5.4 waters (66% RH) up to 9.4 waters per lipid (93% RH), the bromine position gradually decreases from $Z_{Br} = 7.97 \pm 0.27$ Å to $Z_{Br} = 6.59 \pm 0.15$ Å, while A_{Br} increases from 4.62 ± 0.62 Å up to 5.92 ± 0.37 Å. This behavior is consistent with the expected increase in thermal disorder with increasing hydration that causes a decrease in hydrocarbon thickness and increase in the area per lipid molecule. These changes in the double-bond distribution were anticipated by Wiener and White (1992). Just after the hydration shell of the phosphocholine headgroup is filled at ~12 water molecules per lipid (60% PVP), Z_{Br} increases to $\sim \pm 7.3$ Å while A_{Br} decreases to 5.3 Å. This suggests that a discrete structural change takes place when the hydration shell becomes filled, consistent with NMR measurements of the order parameters of the phosphocholine methylenes (Bechinger and Seelig, 1991). In the range 12–16 waters/lipid, the bromine distributions are practically overlapping (Table 1). The average of the Gaussian parameters for the three hydrations are $Z_{Br} = 7.33 \pm 0.25$ Å and $A_{Br} = 5.35 \pm 0.5$ Å.

Although the positions of the Gaussians of the bromine-label distribution correspond exactly with the double-bond distribution, the widths of the bromine-label Gaussians are slightly larger than the actual double-bond because the diameter of the bromines, which is convoluted with the thermal envelope of the double-bonds, is larger than the diameter of the double-bond hydrogens [see Wiener et al. (1991)]. The 1/e half-width of the double-bonds at 66% RH, obtained from specifically deuterated DOPC in neutron scattering experiments, is $A_{C=C} = 4.29 \pm 0.16$ Å compared to $A_{Br} = 4.96 \pm 0.62$ Å. The difference in the two widths is only due to differences in the hard-sphere radii and does not depend on hydration. We have estimated the widths of the double-bond distributions from A_{Br} using the method of Wiener et al. (1991). The widths $A_{C=C}$ are included in Table 1.

The changes in the parameters of the bromine (and double-bond) distribution are modest over the range of hydrations studied, and especially above 76% RH. This finding is consistent with the idea that the changes in the bilayer with hydration are fairly small (McIntosh and Simon, 1986). Nevertheless, our measurements indicate that changes do occur, consistent with the recent NMR measurements of Gawrisch and his colleagues (Koenig et al., 1997). Fig. 6 *B* suggests that the changes in Z_{Br} and A_{Br} are inversely related. This may reflect volumetric constraints on HC of the lipid bilayer. Such constraints may be of value in the development of scaling methods for hydrations in excess of 16 waters/lipid for which $h_{obs} \leq 3$ (Table 1).

DISCUSSION

Scaling of x-ray structure factors

We have obtained relative-absolute (per lipid) structure factors for DOPC over the hydration range of 6.2 to 15.9 waters/lipid using specific bromination of the double-bonds and a modification of the scaling procedure of Wiener and White (1991b), who obtained per-lipid structure factors for DOPC with 5.4 waters/lipid. This represents significant and encouraging progress toward determining the complete and fully resolved structure of fluid bilayers over a wide range of hydrations using joint refinement of x-ray and neutron data (Wiener and White, 1991b). Our set of correctly, and

TABLE 2 Relative-absolute structure factors, $\tilde{F}^*(h) \times 10^{12}$, for hydrations of 6.2 to 15.9 waters/lipid

Hydration Conditions*	W/L[#]	$h = 1$	$h = 2$	$h = 3$	$h = 4$	$h = 5$	$h = 6$
76% RH	6.2	−39.57	−1.78	7.83	−11.41	2.49	−2.58
86% RH	7.7	−39.90	−3.25	8.39	−14.11	2.89	−2.82
93% RH	9.4	−33.09	−2.76	6.80	−9.88	2.09	−2.07
60% PVP	12.0	−37.73	−5.92	10.10	−11.70	—	—
50% PVP	13.6	−39.55	−11.45	15.33	−12.16	—	—
40% PVP	14.2	−36.42	−14.47	15.17	−8.87	—	—
30% PVP	15.9	−34.78	−17.51	16.05	−7.37	—	—

*Samples hydrated through the vapor by equilibration with saturated salt solutions indicated by % RH (oriented samples) and by dispersal in bulk PVP solutions with wt % PVP indicated (unoriented samples).
[#]Waters per lipid. See footnote # of Table 1.

unambiguously, scaled structure factors also provides an opportunity to examine scaling methods that are traditionally used in membrane diffraction.

These traditional methods rely heavily upon the so-called continuous Fourier transform, which is the reciprocal space (structure factor) representation of a single unit cell (lipid bilayer profile). The continuous structure factor is plotted in this representation against the amplitude of the reciprocal space vector $\mathbf{S} = 2 \sin \theta/\lambda$ where λ is the wavelength of the x-rays. The structure factors of order h obtained from

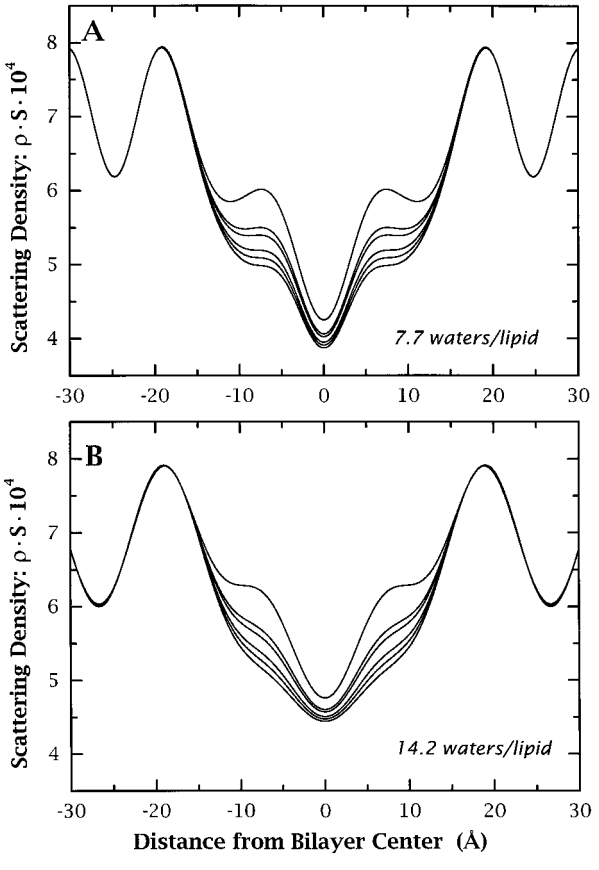

FIGURE 3 Scattering density profiles of DOPC/OBPC bilayers on the relative absolute (per lipid) scale for 0, 5, 10, 20, 25, and 50 mol % OBPC. The Fourier series are generated from the best relative absolute structure factors (see Fig. 1). (*A*) Six-order reconstruction for 86% RH (7.7 waters/lipid). (*B*) Four-order reconstruction for 40% PVP (14.2 waters/lipid). The units are scattering length per length represented here as $\rho^*(z) \cdot S$ (see Eq. 4) to indicate that division by the area/lipid S will place the profiles on the absolute scattering density scale. The two peaks, located at ~7 Å from the bilayer center, increase with increasing amounts of OBPC and are easily identified as the transbilayer distribution of the bromine atoms.

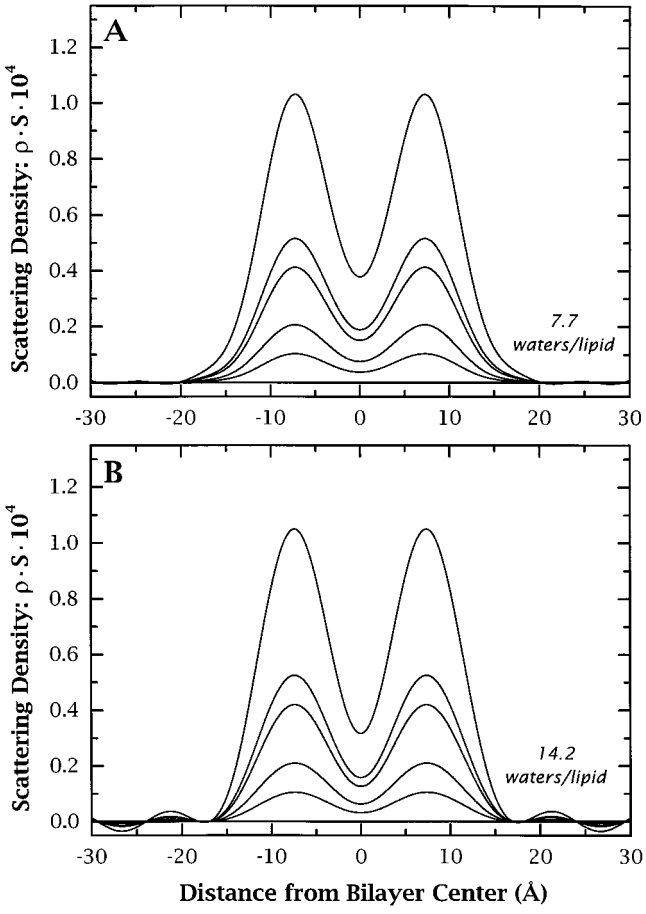

FIGURE 4 Difference scattering-density profiles obtained from the structure factors of the profiles presented in Fig. 3. (*A*) Six-order reconstruction for 86% RH (7.7 waters/lipid). (*B*) Four-order reconstruction for 40% PVP (14.2 waters/lipid). The peaks increase with increasing OBPC content. Note the Fourier noise extending from 20 to 30 Å from the bilayer center. This noise causes the scaling procedure of Wiener and White (1991b) to be inaccurate. The modified procedure presented in the Methods is not affected by this noise (see text)

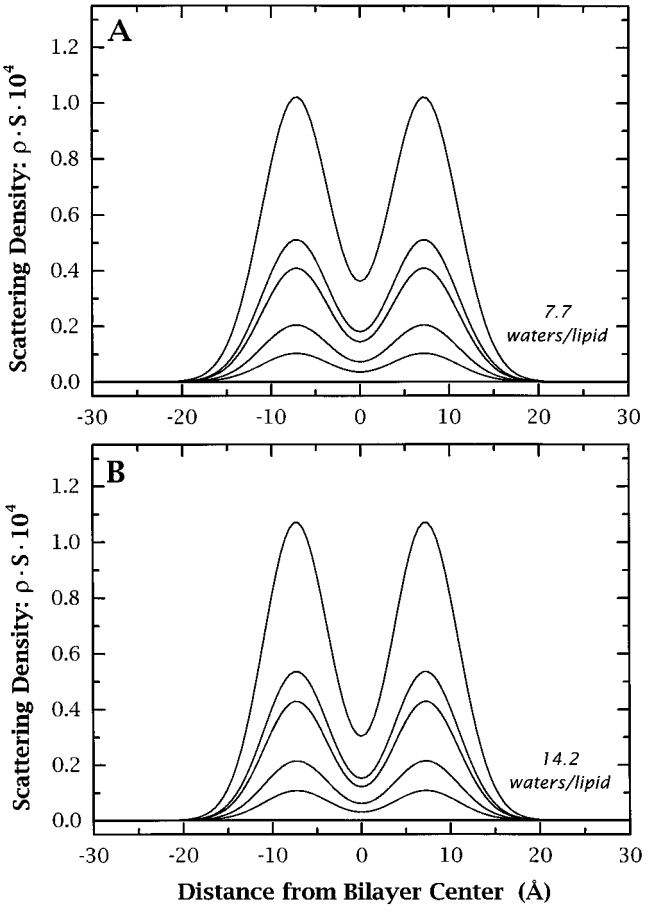

FIGURE 5 Gaussian fits of the difference Fourier profiles presented in Fig. 4 according to the scaling method developed in Materials and Methods. The principal difference between these distributions and those of Fig. 4 is the absence of Fourier noise.

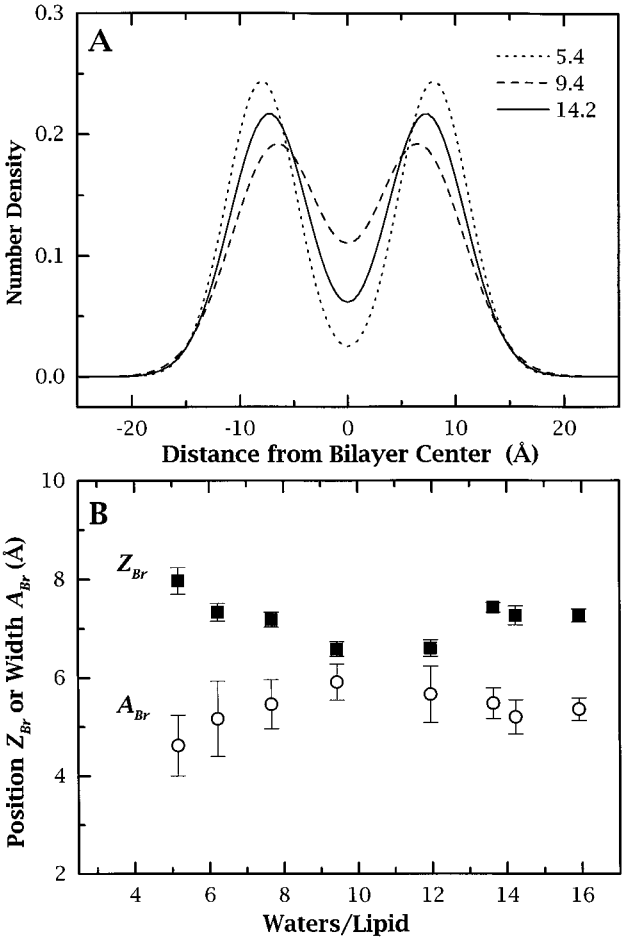

FIGURE 6 Summary of the transbilayer distribution of the bromine-labeled double-bonds in OBPC/DOPC bilayers as a function of hydration. (*A*) Distribution of bromine labels for three characteristic hydrations: 5.4, 9.4, and 14.2 waters/lipid. (*B*) Positions and widths of the Gaussian bromine distributions for hydrations from 5.4 to 16 water molecules per lipid. For hydrations from 5.4 waters (66% RH) up to 9.4 waters/lipid (93% RH), the bromine position gradually decreases from $Z_{Br} = 7.97 \pm 0.27$ Å to $Z_{Br} = 6.59 \pm 0.15$ Å, while A_{Br} increases from 4.62 ± 0.62 Å up to 5.92 ± 0.37 Å. After the hydration shell is filled at ~12 waters/lipid (60% PVP), we observe a shift in Z_{Br} to ~7.3 Å, while A_{Br} decreases to 5.3 Å, suggesting that some structural change takes place at the point of completion of the hydration shell.

multilamellar samples with N bilayers are derived mathematically from the continuous transform by convoluting it with a perfect-lattice function consisting of N delta functions spaced at intervals of d along the z-axis [see review by Franks and Levine (1981)]. This convolution causes the continuous transform to be sampled at $\mathbf{S} = h/d$. The values of the continuous structure factor obtained at these sampled points correspond to the structure factors obtained from multilamellar samples.

The relative-absolute continuous Fourier transforms for DOPC calculated using the Shannon sampling theorem (Worthington et al., 1973) are shown in Fig. 7 *A* for 5.4 waters/lipid (*solid curve*) and 15.9 waters/lipid (*dashed curve*). The data points are the structure factors for all hydrations studied (5.4 to 15.9 waters/lipid). Presentation of the data in this manner provides an opportunity to check the consistency of the scaling at different hydrations and to understand the qualitative behavior of the continuous transform at different water contents. To address these issues, we modeled the change in the continuous transform of the unit cell of the bilayer by adding water between bilayers whose structure is known at low hydrations. Specifically, we added 10.5 waters/lipid distributed as a Gaussian to the 66% RH DOPC bilayer structure (Wiener and White, 1992) such that the d-spacing increased by 6 Å. This model is only approximate because 1) we assume that the bilayer structure does not change as a function of hydration (which is not exactly true, see Fig. 6); and 2) we have no detailed structural information about the distribution of water at hydrations above 66% RH (in principle it can be obtained from neutron diffraction experiments). Thus, the only requirement of the model was that the sum of the bilayer scattering profile at 66% RH (*dotted line*, Fig. 7 *B, inset*) and the newly added water (*dashed line*, Fig. 7 *B, inset*) be smooth and resemble qualitatively a profile at higher hydrations (*solid line*, Fig. 7 *B, inset*). This model cannot be used for exact predictions,

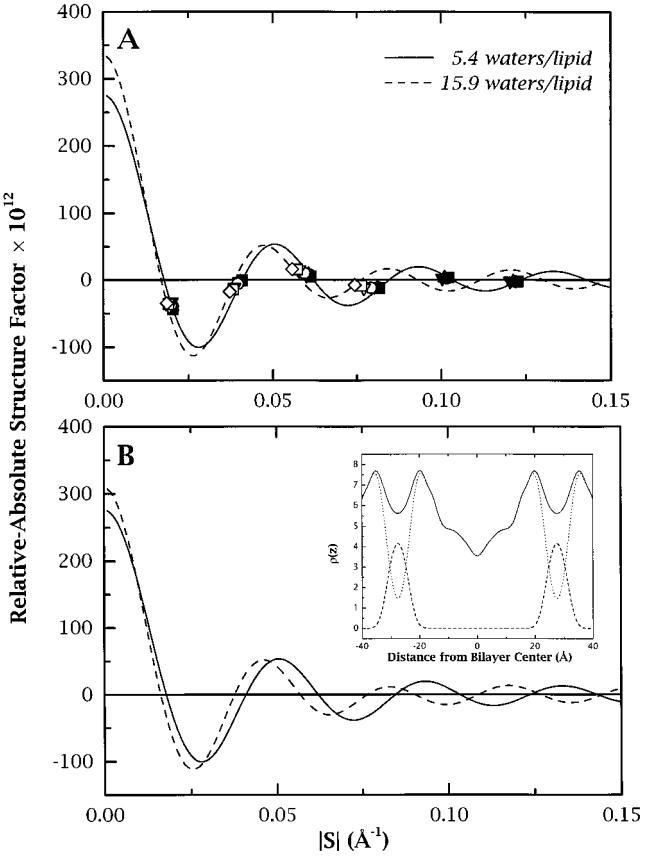

FIGURE 7 Observed and model continuous transforms of DOPC bilayers for different hydrations. The continuous transforms, calculated using the Shannon sampling theorem, are the continuous structure factors of a bilayer unit cell plotted against the magnitude of the reciprocal space vector, $|\mathbf{S}| = 2 \sin \theta/\lambda$. In diffraction from a multilamellar bilayer system, this transform is sampled at values of $|\mathbf{S}| = h/d$ to produce structure factors of order h (see text); d is the Bragg spacing. (*A*) Observed continuous relative-absolute structure factors for pure DOPC bilayers at different hydrations. The solid and the dotted lines are the continuous transforms for 66% RH (5.4 waters/lipid) and 30% PVP (15.9 waters/lipid), respectively. The data points are the observed discrete structure factors covering the same hydration range. (*B*) Model continuous transforms for the DOPC bilayer at two hydrations based upon the known (Wiener and White, 1992) complete structure of DOPC at 5.4 waters/lipid. The solid line is the continuous transform for DOPC at 5.4 waters/lipid (*A*) and the dashed line the continuous transform calculated for 15.9 waters/lipid from the model. The prediction of the model is in excellent qualitative agreement with the 15.9 water/lipid transform of (*A*). *Inset:* Summary of the model used to calculate the 10.5 waters/lipid transform. The model bilayer profile (*solid curve*) is the sum of the bilayer profile at 66% RH (*dotted line*) and additional Gaussian-distributed 11.4 waters/lipid (*dashed line*).

but it does provide a qualitative idea about the behavior of the continuous transform of the bilayer as hydration is increased. In Fig. 7 *B*, the continuous transform of the hydrated bilayer at 66% RH (5.4 waters/lipid) is shown as the solid line and the transform of the model (15.9 waters/lipid) as a dashed line. The observed and model transforms of Fig. 7, *A* and *B*, respectively, are in excellent agreement and therefore indicative of consistent scaling.

The discussion of our scaling procedure in the Methods indicates the complex nature of the scaling of membrane diffraction data. In the absence of isomorphous-labeling data, x-ray data obtained in separate experiments at different hydrations are treated by means of the so-called minus-fluid ($-F$) bilayer model (Worthington et al., 1973; Worthington, 1981). The underlying assumption (Worthington et al., 1973) is that the bilayer unit cell can be subdivided in two parts: a bilayer with an electron density distribution $\rho_b(z)$ and thickness d_b and a fluid (water) layer of uniform electron density F and thickness d_w. The $-F$ model is defined as a bilayer with an electron density distribution $\rho_b(z) - F$ so that the "water layer" of the $-F$ model now has an electron density of zero. Because the electron density of the water layer in the $-F$ model is 0, the 0th order is given by $\rho_b d_b + 0 \cdot d_w$, and thus does not depend on d_w. This procedure can be better understood in the context of Eqs. 4 and 5. In the $-F$ model, the mean electron density is given by

$$\rho^*_{0(-F)} = \rho^*_0 - \frac{2}{d}\left(n_w b_w - \frac{V_{lip}}{V_w} b_w\right) = \frac{2}{d}\left(b_{lip} - \frac{V_{lip}}{V_w} b_w\right) \quad (18)$$

where V_{lip} and V_w are the molecular volumes of the lipid and water, respectively. From Eq. 4, the 0th diffraction order can be defined formally as

$$\rho^*_{0(-F)} d = 2\left(b_{lip} - \frac{V_{lip}}{V_w} b_w\right) \quad (19)$$

Equation 19 does not contain d_w and is therefore constant for all hydrations. Consequently, changes in d_w have no effect on the continuous transform of the unit cell. This procedure causes the amplitude of the continuous transforms for all hydrations to have the same value at the origin ($|\mathbf{S}| = 0$). Conveniently, the 0th order of pure unbrominated bilayers generally has a value of approximately 0. Thus, if this "dehydrated" bilayer structure of the $-F$ model does not change with hydration, all structure factors measured at different d_w will fall on a single continuous transform.

To use the $-F$ model in the absence of absolute scaling, the x-ray data sets from the measurements at different hydrations must be placed on a common, but arbitrary scale. This is generally done using a formula introduced by Blaurock (Blaurock and Stoeckenius, 1971; McIntosh and Simon, 1986):

$$\sum_h \frac{f_h^2}{d} = \text{constant} \quad (20)$$

The sum must formally include the 0th order, but since the 0th order is practically zero for most lipids, its inclusion has little effect. This scaling, adopted specifically for the $-F$ model, assumes that the bilayer doesn't change with hydration (which is not true, Fig. 6), and it is unconnected from the absolute variations of scattering density around the mean density. Furthermore, the sum can extend only over the observed structure factors that vary in number from 4 to 8 in our experiments. Thus, there is no reason to expect that our relative-absolute structure factors will satisfy Eq. 20. Yet, the scaled values of $\sqrt{\Sigma F^2/d^2}$, as shown in Table 1, are

almost identical within experimental error. This is due to the fact that the sum is dominated by the extremely strong first-order structure factor.

We examined our results in the context of the $-F$ model in two ways: 1) we used our relative-absolute structure factors (Table 2) without further scaling, and 2) our experimental structure factors scaled according to Eq. 20. Because our relative-absolute structure factors have already been scaled and because the $-F$ model is set up to remove the dependence of the bilayer profile on the 0th order, our $\tilde{F}^{*}_{B}(h)$ are the structure factors for the $-F$ model of DOPC. The continuous transform constructed from our relative-absolute structure factors are shown in Fig. 8 *A*. The solid line is the sampling-theorem reconstruction for 76% RH (6.2 waters) (Shannon, 1949; Jerri, 1977; Worthington, 1988). All of the structure factors fall close to this line. As expected, the fit is not perfect because of the changes in the bilayer structure with hydration. Interestingly, however, as shown in Fig. 8 *B*, the continuous transform of the $-F$ model applied in the traditional way to our unscaled structure factors is remarkably similar to that of Fig. 8 *A*. Thus, the $-F$ model appears to provide an adequate description of the continuous transform, but on an arbitrary scale. This makes it useful for verifying the phases of the structure factors.

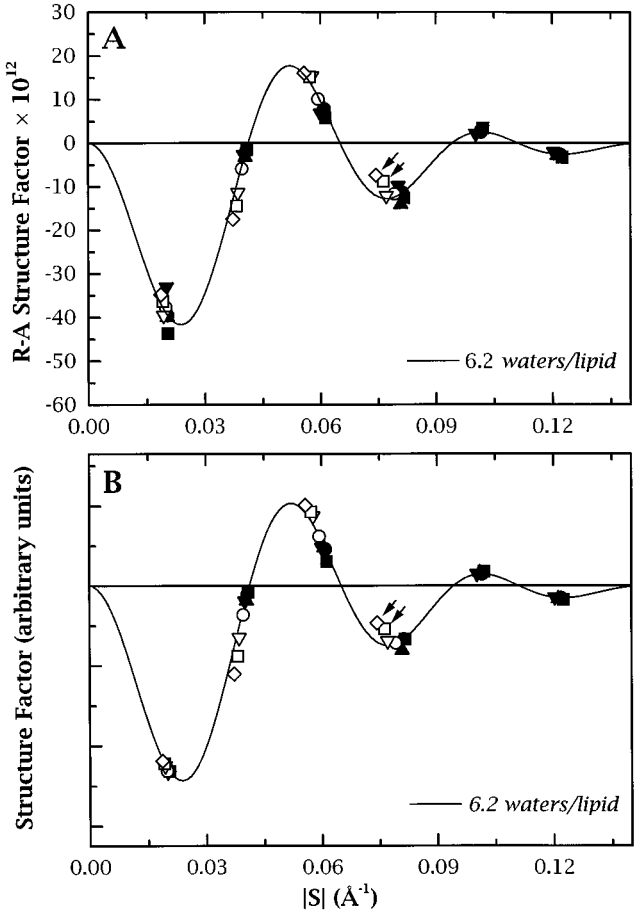

FIGURE 8 Continuous transforms based on the so-called fluid-minus ($-F$) model using relative-absolute (R-A) and arbitrary-scale structure factors. The $-F$ model is described in detail in the text. (*A*) Continuous relative-absolute structure factors for hydrations of 5.4 to 16 waters/lipid. The solid line is the continuous transform for the minus fluid model (Worthington et al., 1973) for 76% RH. The data points are the observed discrete structure factors. The structure factors at the highest hydrations studied do not deviate substantially from the solid line, which indicates that there is no substantial loss of diffracted intensity due to lattice disorder (see text). Only the fourth orders for 14.2 and 15.9 waters/lipid (*arrows*) show evidence of possible dampening due to membrane undulations. (*B*) Continuous structure factors on an arbitrary scale that have been scaled according to Blaurock (1971), Eq. 20. The solid line is the continuous transform for the $-F$ model for 76% RH.

Bilayer undulations

The canonical resolution of the diffraction experiment is d/h_{max}, where d is the Bragg spacing and h_{max} is the maximum possible number of diffraction orders. For our measurements, d is 50–60 Å and h_{max} is 4–8, so that our canonical resolution varies from 6 to 12 Å. [One should not confuse this resolution with the "resolution precision" (White and Wiener, 1995) that describes the precision with which the position of a fully resolved feature, such as the bromine-labeled double-bonds, can be determined. The uncertainty of the position of the double-bonds in our experiments is only ~0.2 Å (Table 1).] If the bilayers are oriented and the lattice excellent, then $h_{obs} = h_{max}$ and the image of the unit cell is a fully resolved one. With high degrees of orientational disorder, as in the powder patterns obtained using PVP solutions, the intensities can be spread so thinly that the signal drops below the noise level. In that case, $h_{obs} < h_{max}$ and the unit cell image is under-resolved. Another issue that arises with unoriented multilayers in the presence of excess PVP solutions is lattice disorder caused by bilayer undulations that can also, or in addition, cause $h_{obs} < h_{max}$. These undulations lead to broad non-Bragg scattering peaks with long power-law tails. The intensities of the broad "wings" of the peaks can consequently become smaller than the background noise (Nagle et al., 1996), causing the higher orders to be underestimated. This underestimation will introduce error in the scaling of the data. We therefore needed to be sure that all the intensity in the diffracted peaks was collected in order to claim that the double-bond distribution is determined correctly. To detect lattice disorder, however, a highly monochromatic x-ray beam and high-resolution detector must be used (Zhang et al., 1996). Our experimental system lacked the resolution required for such measurements.

A way to distinguish whether all the diffracted intensity is recovered is to examine the continuous transform in the $-F$ model (Fig. 8). If signal is being lost, then the high-order structure factors at high hydrations should be smaller than predicted from the continuous transform calculated from the structure factors at lower hydrations. Inspection of Fig. 8 suggests that it is possible that the fourth orders for 14–16 waters/lipid (indicated by *arrows*) are dampened due to the membrane undulations. By comparing the experimentally

determined and anticipated values from the continuous transform, we determined the possible effect of the fluctuations, and then applied the scaling procedure to the corrected structure factors. The values of $Z_{Br} = 7.33 \pm 0.25$ Å and $A_{Br} = 5.35 \pm 0.50$ Å for 12–16 waters/lipid changed to 7.11 and 5.16 Å, respectively, when corrected for possible fluctuations. The differences are within experimental error, and we conclude that below 16 waters/lipid membrane fluctuations are not large enough to cause a substantial loss of diffracted intensity, and thereby substantially alter results presented in Table 1 and Fig. 6.

Effect of hydration on the transbilayer distribution of double-bonds

Our results show that the bromine distribution in OBPC/DOPC bilayers, which reports the double-bond distribution in DOPC bilayers, changes with hydration up to the point of completion of the hydration shell at ~12 waters/lipid. At higher hydrations (12–16 waters/lipid), the bromine distribution remains constant at $Z_{Br} = 7.33 \pm 0.25$ Å and $A_{Br} = 5.35 \pm 0.5$ Å, consistent with NMR studies (Bechinger and Seelig, 1991; Koenig et al., 1997). The changes in the parameters of the bromine distribution are, however, modest over the studied range of hydrations, and especially above 76% RH.

An interesting question is that of the effect of hydration on the distribution of the double-bonds within the hydrocarbon volume. The complete solution of the bilayer structure at 66% RH (Wiener and White, 1992) allowed the comparison of the distributions of the different quasimolecular fragments in the hydrocarbon region. The width of the double-bond distribution was found to be significantly larger than the widths of the terminal methyl groups, the carbonyl, or the phosphate group (Wiener and White, 1992). This may be because restricted motions of the methyl and carbonyl groups make the chains behave as if they are tethered at the water interface and the bilayer midplane such that the double-bond diffuses over a large volume of the hydrocarbon chain. In any case, the full extent of the double-bond distribution included much of the HC thickness.

How is the occupancy of the HC volume affected by increases in hydration? Wiener and White (1992) showed that at 66% RH (5.4 waters/lipid), the positions of the choline, phosphate, glycerol, and carbonyl groups coincide precisely with certain thicknesses determined from simple volumetric calculations of bilayer thickness used by Luzzati and Husson (1962), Small (1967), and Nagle and Wiener (1988). Assuming that the packing density of the lipid bilayer is invariant with hydration, as seems likely (Petrache et al., 1997), then such volumetric considerations will be applicable to the bilayer structure at all hydrations. The volumetric predictions for the position of the carbonyl moiety as a function of hydration, based upon our measurements of the Bragg spacing (Table 1), are shown in Fig. 9 as solid squares. The open square is the position of the carbonyls determined by Wiener and White (1992) for 5.4 waters/lipid. Wiener and White (1992) also showed that the transbilayer carbonyl-to-carbonyl distance accurately reported the thickness D_{HC} of the hydrocarbon core. The break in the Bragg spacing at 11.6 waters/lipid indicates the completion of the phosphocholine hydration shell. Shown in

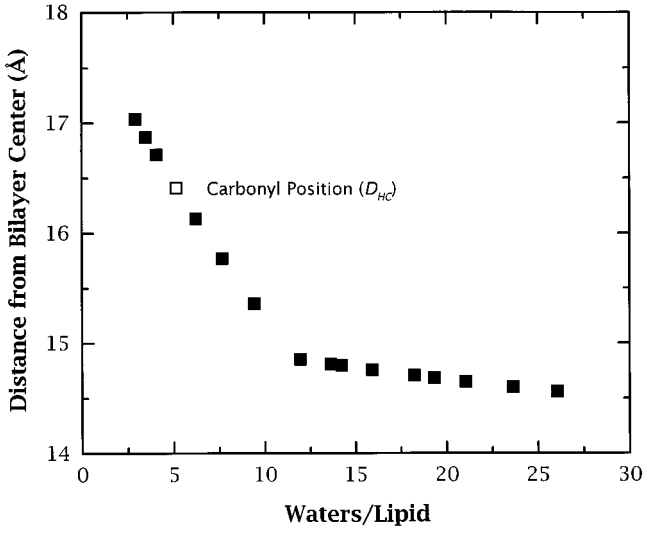

FIGURE 9 Calculated and measured positions of the carbonyl groups of DOPC as a function of hydration. The calculated positions (D_{HC}, ■) are derived from volumetric considerations using the formulas of Nagle and Wiener (1988) using our measured values of *d*-spacing and the number of water molecules per lipid (McIntosh et al., 1987). The open symbol (□) is the position determined by Wiener and White (1992) using liquid-crystallography

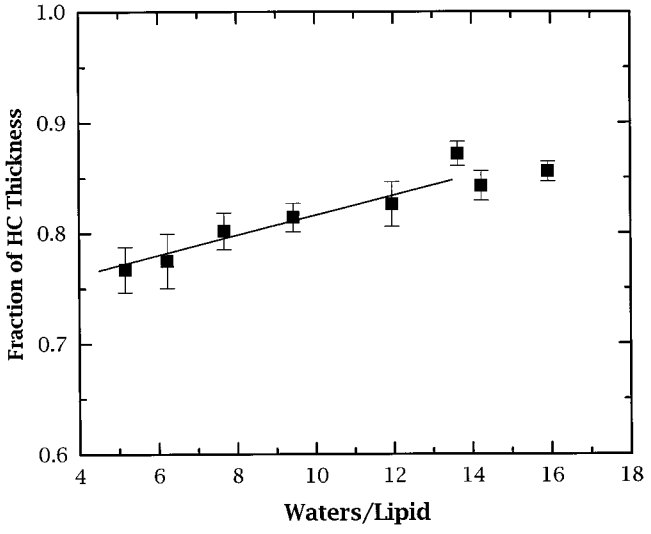

FIGURE 10 Estimated fraction of the hydrocarbon core thickness D_{HC} of DOPC explored by the brominated double-bonds as a function of hydration. The fraction explored is calculated from $2(Z_{Br} + A_{Br})/D_{HC}$. The solid symbols (■) correspond to 5.4 to 16 waters per lipid. The accessible volume increases with hydration, at least until the hydration shell is filled at ~12 waters/lipid, which is an indication of increased thermal motion within the bilayer. The solid line is the linear fit for hydrations of 5.4–12 waters/lipid.

Fig. 10 is the hydration dependence of the hydrocarbon volume that is accessible to bromine calculated from $2(Z_{Br} + A_{Br})/D_{HC}$. The solid symbols (■) correspond to hydrations of 5.4 to 16 waters per lipid for which the bromine distribution was determined. The accessible volume of the double-bonds clearly increases with hydration, at least until the hydration shell is filled, as expected from the increased thermal motion that accompanies increased hydration.

Further understanding of the behavior of the hydrocarbon core at hydrations higher than 16 waters/lipid can be achieved only after the x-ray data at high hydrations are scaled and the double-bond distribution determined. New scaling methods are needed for this purpose.

We thank Drs. Tom McIntosh, Michael Wiener, John Nagle, and Stephanie Tristram-Nagle for their comments on the manuscript and Dr. Klaus Gawrisch for sharing the results of his NMR measurements before publication.

This work was supported in part by National Institutes of Health Grants GM-46823 (to S.H.W.) and AI-31696 and AI-22931 (to Michael E. Selsted).

REFERENCES

ASTM Standards. 1952. Recommended practice for maintaining constant relative humidity by means of aqueous solutions. *In* Book of ASTM Standards, Part 6. American Society for Testing Materials, Philadelphia. 706–710.

Barlow, R. J. 1989. Statistics. A Guide to the Use of Statistical Methods in the Physical Sciences. John Wiley and Sons, New York. 1–204.

Barton, P. G., and F. D. Gunstone. 1975. Hydrocarbon chain packing and molecular motion in phospholipid bilayers formed from unsaturated lecithins. *J. Biol. Chem.* 250:4470–4476.

Bechinger, B., and J. Seelig. 1991. Conformational changes of the phosphatidylcholine headgroup due to membrane dehydration: a ^{2}H-NMR study. *Chem. Phys. Lipids*. 58:1–5.

Blaurock, A. E., and W. Stoeckenius. 1971. Structure of the purple membrane. *Nature New Biol.* 233:152–155.

Boden, N., S. A. Jones, and F. Sixl. 1991. On the use of deuterium nuclear magnetic resonance as a probe of chain packing in lipid bilayers. *Biochemistry*. 30:2146–2155.

Franks, N. P., T. Arunachalam, and E. Caspi. 1978. A direct method for determination of membrane electron density profiles on an absolute scale. *Nature (Lond.)*. 276:530–532.

Franks, N. P., and Y. K. Levine. 1981. Low-angle x-ray diffraction. *In* Membrane Spectroscopy. E. Grell, editor. Springer-Verlag, Berlin. 437–487.

Franks, N. P., and W. R. Lieb. 1979. The structure of lipid bilayers and the effects of general anesthetics: an x-ray and neutron diffraction study. *J. Mol. Biol.* 133:469–500.

Gibbs, J. W. 1898a. Fourier's series. *Nature (Lond.)*. 59:200.

Gibbs, J. W. 1898b. Fourier's series. Correction. *Nature (Lond.)*. 59:606.

Helfrich, W. 1973. Elastic properties of lipid bilayers: theory and possible experiments. *Z. Naturforsch. C*. 28:693–703.

Hosemann, R., and S. N. Bagchi. 1962. Direct Analysis of Diffraction by Matter. North-Holland, Amsterdam. 1–734.

Jacobs, R. E., and S. H. White. 1987. Lipid bilayer perturbations induced by simple hydrophobic peptides. *Biochemistry.* 26:6127–6134.

Jacobs, R. E., and S. H. White. 1989. The nature of the hydrophobic binding of small peptides at the bilayer interface: implications for the insertion of transbilayer helices. *Biochemistry*. 28:3421–3437.

Jerri, A. J. 1977. The Shannon sampling theorem—its various extensions and applications: a tutorial review. *IEEE Proc.* 65:1565–1596.

King, G. I., R. E. Jacobs, and S. H. White. 1985. Hexane dissolved in dioleoyllecithin bilayers has a partial molar volume of approximately zero. *Biochemistry*. 24:4637–4645.

King, G. I., and S. H. White. 1986. Determining bilayer hydrocarbon thickness from neutron diffraction measurements using strip-function models. *Biophys. J.* 49:1047–1054.

Koenig, B. W., H. H. Strey, and K. Gawrisch. 1997. Membrane lateral compressibility determined by NMR and x-ray diffraction: effect of acyl chain polyunsaturation. *Biophys. J.* in press

LeNeveu, D. M., R. P. Rand, V. A. Parsegian, and D. Gingell. 1977. Measurement and modification of forces between lecithin bilayers. *Biophys. J.* 18:209–230.

Levine, Y. K., and M. H. F. Wilkins. 1971. Structure of oriented lipid bilayers. *Nature New Biol.* 230:69–72.

Luzzati, V., and F. Husson. 1962. The structure of the liquid-crystalline phases of lipid-water systems. *J. Cell Biol.* 12:207–219.

McIntosh, T. J., A. D. Magid, and S. A. Simon. 1987. Steric repulsion between phosphatidylcholine bilayers. *Biochemistry*. 26:7325–7332.

McIntosh, T. J., A. D. Magid, and S. A. Simon. 1989. Repulsive interactions between uncharged bilayers: hydration and fluctuation pressures for monoglycerides. *Biophys. J.* 55:897–904.

McIntosh, T. J., and S. A. Simon. 1986. Hydration force and bilayer deformation: a reevaluation. *Biochemistry*. 25:4058–4066.

Nagle, J. F., and M. C. Wiener. 1988. Structure of fully hydrated bilayer dispersions. *Biochim. Biophys. Acta*. 942:1–10.

Nagle, J. F., R. Zhang, S. Tristram-Nagle, W. Sun, H. I. Petrache, and R. M. Suter. 1996. X-ray structure determination of fully hydrated L_α phase dipalmitoylphosphatidylcholine bilayers. *Biophys. J.* 70: 1419–1431.

O'Brien, F. E. M. 1948. The control of humidity by saturated salt solutions. *Rev. Sci. Instrum.* 25:73–76.

Parsegian, V. A., R. P. Rand, N. L. Fuller, and D. C. Rau. 1986. Osmotic stress for the direct measurement of intermolecular forces. *Methods Enzymol.* 127:400–416.

Petrache, H. I., S. E. Feller, and J. F. Nagle. 1997. Determination of component volumes of lipid bilayers from simulations. *Biophys. J.* 70:2237–2242.

Sakurai, I., S. Iwayanagi, T. Sakurai, and T. Seto. 1977. X-ray study of egg-yolk lecithin: unit cell data and electron density profile. *J. Mol. Biol.* 117:285–291.

Shannon, C. E. 1949. Communications in the presence of noise. *Proc. Inst. Radio Engrs.* 37:10–21.

Sirota, E. B., G. S. Smith, C. R. Safinya, R. J. Plano, and N. A. Clark. 1988. X-ray scattering studies of aligned, stacked surfactant membranes. *Science*. 242:1406–1409.

Small, D. M. 1967. Phase equilibria and structure of dry and hydrated egg lecithin. *J. Lipid Res.* 8:551–557.

Small, D. M. 1986. The Physical Chemistry of Lipids. Plenum Press, New York. 1–672.

Suwalsky, M., and L. Duk. 1987. Structure determination of oriented films of L-α-dimyristoylphosphatidylethanolamine (DMPE). *Makromol. Chem.* 188:599–606.

Torbet, J., and M. H. F. Wilkins. 1976. X-ray diffraction studies of lecithin bilayers. *J. Theor. Biol.* 62:447–458.

Warren, B. E. 1969. X-ray Diffraction. Addison-Wesley, Reading, MA. 1–381.

White, S. H., R. E. Jacobs, and G. I. King. 1987. Partial specific volumes of lipid and water in mixtures of egg lecithin and water. *Biophys. J.* 52:663–665.

White, S. H., and M. C. Wiener. 1995. Determination of the structure of fluid lipid bilayer membranes. *In* Permeability and Stability of Lipid Bilayers. E. A. Disalvo and S. A. Simon, editors. CRC Press, Boca Raton. 1–19.

White, S. H., and M. C. Wiener. 1996. The liquid-crystallographic structure of fluid lipid bilayer membranes. *In* Membrane Structure and Dynamics. K. M. Merz and B. Roux, editors. Birkhäuser, Boston. 127–144.

Wiener, M. C., G. I. King, and S. H. White. 1991. Structure of a fluid dioleoylphosphatidylcholine bilayer determined by joint refinement of x-ray and neutron diffraction data. I. Scaling of neutron data and the distribution of double-bonds and water. *Biophys. J.* 60:568–576.

Wiener, M. C., and S. H. White. 1991a. Fluid bilayer structure determination by the combined use of x-ray and neutron diffraction. I. Fluid bilayer models and the limits of resolution. *Biophys. J.* 59:162–173.

Wiener, M. C., and S. H. White. 1991b. Fluid bilayer structure determination by the combined use of x-ray and neutron diffraction. II. "Composition-space" refinement method. *Biophys. J.* 59:174–185.

Wiener, M. C., and S. H. White. 1991c. Transbilayer distribution of bromine in fluid bilayers containing a specifically brominated analog of dioleoylphosphatidylcholine. *Biochemistry*. 30:6997–7008.

Wiener, M. C., and S. H. White. 1992. Structure of a fluid dioleoylphosphatidylcholine bilayer determined by joint refinement of x-ray and neutron diffraction data. III. Complete structure. *Biophys. J.* 61: 434–447.

Worthington, C. R. 1981. The determination of the first-order phase in membrane diffraction using electron density strip models. *J. Appl. Crystallogr.* 14:387–391.

Worthington, C. R. 1988. Sampling-theorem expressions in membrane diffraction. *J. Appl. Crystallogr.* 21:322–325.

Worthington, C. R., G. I. King, and T. J. McIntosh. 1973. Direct structure determination of multilayered membrane-type systems which contain fluid layers. *Biophys. J.* 13:480–494.

Wu, Y., K. He, S. J. Ludtke, and H. W. Huang. 1995. X-ray diffraction study of lipid bilayer membranes interacting with amphiphilic helical peptides: diphytanoyl phosphatidylcholine with alamethicin at low concentrations. *Biophys. J.* 68:2361–2369.

Zhang, R.-T., S. Tristram-Nagle, W.-J. Sun, R. L. Headrick, T. C. Irving, R. M. Suter, and J. F. Nagle. 1996. Small-angle x-ray scattering from lipid bilayers is well described by modified Caillé theory but not by paracrystalline theory. *Biophys. J.* 70:349–357.